Effect of H_2O-CO_2 Organization on Ovalbumin Adsorption at the Supercritical CO_2−Water Interface

Frederic Tewes and Frank Boury*

Ingénierie de la Vectorisation Particulaire, INSERM U 646, Bat. IBT, 10 rue A. Boquel, 49100 Angers, France

Received: July 10, 2004; In Final Form: September 20, 2004

We have studied the formation of water−CO_2 interfaces in the presence of different concentrations of ovalbumin (OVA) by tensiometry and by means of interfacial rheological measurements to obtain some information on the capacity of protein film to stabilize H_2O in CO_2 emulsion. The formation of pure water−CO_2 interface can be described as a two-step phenomenon.[1] The CO_2 molecules adsorb onto the water surface and then a reorganization of the interface creates a H_2O-CO_2 cluster network. This organization occurs at a temperature (40 °C) higher than the higher temperature limit (10 °C) allowing the formation of crystalline structure called CO_2 clathrate.[2] Our results show that ovalbumin adsorption from bulk concentrations higher than 0.0229 g/L inhibits the cluster formation for a CO_2 pressure less than 80 bar. However, for lower concentrations, the more the CO_2 pressure is close to 80 bar, the more OVA adsorption is reduced by the H_2O-CO_2 cluster network. Moreover, from a pressure of 90 bar, the affinity of OVA for the interface increases and mixed films made of protein molecules and clusters are obtained for the OVA concentrations lower than 1 g/L.

Introduction

Supercritical carbon dioxide ($ScCO_2$) is becoming increasingly interesting for many applications such as medium reaction,[3,4] foaming agent, nonmiscible phase for emulsions,[3,5] microemulsions,[6−8] or latexes formation, as well as in cleaning processes.[9] This is due to its peculiar physical properties, which allow the easy tuning of its density and consequently of its solvent power in a small range of temperature and pressure. Moreover, its use answers the need of the substituting toxic and environmentally bad organic solvents in these processes.

In the last 10 years, many studies deal with the formation of water in CO_2 (W/C) and CO_2 in water (C/W) microemulsions[7,8] and emulsions.[5] The first experiments were feasibility studies, with the search of very CO_2-soluble surfactants (i.e., with fluoroalkyl, fluoroether, or siloxane tails). Almost all studies were based on phase behavior, droplet size determination, conductivity, and interfacial tension (γ) measurements.[5,10] However, only a few studies have measured γ between H_2O and CO_2 with surfactant[5,10] while no studies included interfacial rheology.

The dispersed droplets in an emulsion are in constant motion and therefore there are frequent collisions between them in the absence of steric or electrical barrier. These collisions lead to droplet aggregation and, if the interfacial wall is broken, to an irreversible coalescence. In C/W emulsion, this kind of barrier can be created, as this is done in O/W emulsion. Unfortunately, in W/C emulsion, it is very difficult to obtain such a barrier without the use of expensive and unknown biocompatibility surfactants containing fluoroalkyl or fluoroether tails.[11,12] In fact, few polymers able to create a steric barrier are soluble in CO_2, except fluoropolymers, siloxanes, and polycarbonates. Furthermore, the CO_2 has a low dielectric constant, which renders difficult the creation of an electrostatic barrier.

* To whom correspondence should be addressed. E-mail: boury@ibt.univ-angers.fr; phone: +332 41 73 58 48; fax: +332 41 73 58 03.

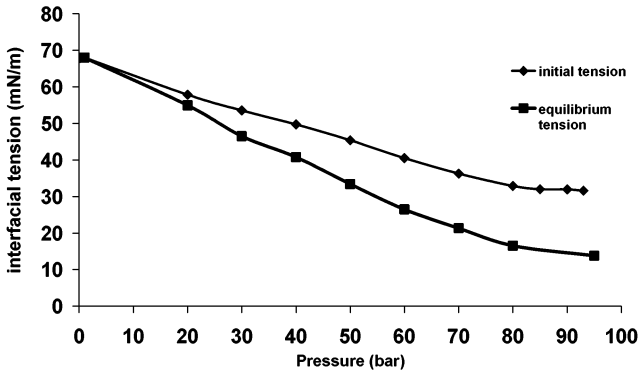

Figure 1. Initial and equilibrium (60 000 s) interfacial tension measured at 40 °C versus pCO_2, from Tewes et al.[1]

Consequently, the mechanical strength of the interfacial film is one of the prime factors determining the stability of the W/C emulsion.

Proteins strongly adsorb at the oil−water interface, often leading to an interfacial layer with an important elastic contribution.[13−15] Such interfacial films could provide suitable properties to stabilize direct or inverse emulsions composed of water and CO_2.

We previously investigated the formation of water−CO_2 (W−C) interface by means of a drop tensiometer, in which one can control the temperature, pressure, and drop area.[1]

In this study, we have measured the initial and equilibrium interfacial tension between water and CO_2 (Figure 1) and we have described the formation of this interface as a two-step phenomenon. First, the CO_2 molecules quickly adsorb onto the water surface for equilibrating their chemical potential between the bulk CO_2 and the water surface. This physisorption leads to the interaction of one CO_2 molecule with one H_2O molecule. From the calculated CO_2 molecular area at saturation and the thermodynamical parameters, we have found that this H_2O-CO_2 complex would be of H type, as it was found by da Rocha

10.1021/jp046940d CCC: $30.25
Published on Web 01/13/2005

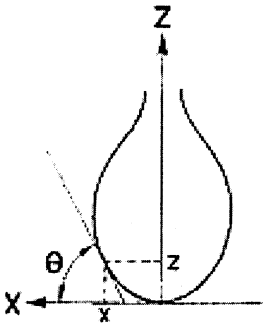

Figure 2. Profile of drop analyzed with Laplace equation.

et al.[16] by Monte Carlos simulation. The amount of adsorbed CO_2 and the relative orientation of water$-CO_2$ molecules in the H type complex depend on temperature and pressure.

Second, after this adsorption, CO_2 molecules diffuse into water and then modify the water molecules organization to create an interphase. This reorganization of the interface creates a network of H_2O-CO_2 clusters and leads to a decrease in the interfacial tension (γ) until an equilibrium state. These H_2O-CO_2 clusters are formed at temperatures higher (20−40 °C) than the one usually described as the limit (10 °C) for the formation of crystalline clathrate hydrate.[2,17,18]

Elasticity measurements and macroscopic visualization suggest that the growing of the clusters is driven by the assembly of many small blocks and accelerates with the CO_2 pressure. Their interfacial concentration and their size increase with time until the saturation of the interface.

This organization of the pure H_2O-CO_2 interface raises an important question. How does the interface react in the presence of usual or polymeric surfactant molecules such as proteins? To answer this question, we have studied the H_2O-CO_2 interface at 40 °C, in the presence of different concentrations of ovalbumin (OVA), and for various CO_2 pressures, by measuring interfacial tension and film elasticities by means of a pendant drop method.

Materials and Methods

Materials. The vessel was filled with CO_2 (purity 0.99) (Air liquide, France). Ultrapure water was produced by MilliQ plus 188 apparatus (Millipore St Quentin en Yveline, France) and then saturated 12 h with pure CO_2. Ovalbumin of grade V was purchased from SIGMA, Germany.

Pendant Drop Tensiometer. The drop tensiometer (Tracker, IT Concept, Longessaigne, France) allows the determination of the interfacial tension by analyzing the axial symmetric shape (Laplacian profile) of the pendant drop of CO_2 saturated water in pressurized CO_2. The apparatus has been described in a previous study.[1] Pendant drops were formed at the end of a stainless steel tube, 1-mm inside diameter, connected to a syringe. Drop volume and area were controlled during all experiments by a step-by-step motor. Therefore, it was possible to maintain constant the area of the drop during the time of the experience, so that the surface tension variation was related only to the adsorption of molecules at the interface.

The interfacial tension was determined by digitizing and analyzing the profile of the droplet (Figure 2) using a CCD camera coupled to a video image profile digitizer board connected to a computer. The drop profile was processed according to the fundamental Laplace equation [eq 1] applied to the drop profile:

$$\frac{1}{x}\frac{d}{dx}(x\sin\theta) = \frac{2}{b} - cz \quad (1)$$

Where x and z are the Cartesian coordinates at any point of the drop profile. b is the radius of the curvature of the drop apex. θ is the angle of the tangent to the drop profile. In addition, c is the capillarity constant, equal to "$(g\rho)/\gamma$", where ρ is the difference between the densities of the two liquids and g is the acceleration due to gravity. Five times per second, the computer calculates the characteristic parameters of the drop (area, volume, and interfacial tension).

Rheological Measurement. Theoretical aspects have been largely developed and discussed in previous papers.[14,19,20] In summary, the viscoelastic response of an interfacial film submitted to a dilatational mechanical strain was studied using a theoretical approach based on two-dimensional rheology.[21]

This approach consists of realizing two types of continuous and monotonic compression of the equilibrated surface layer of a pendant drop: a slow compression and fast compression. We recorded simultaneously the variation of the interfacial tension (i.e., resulting stress) during the slow compression, and after the fast compression, to measure the relaxation of the interface.

In this case, a convenient theoretical model (generalized Maxwell, Figure 3), corresponding to a solid viscoelastic body, is applied and allowed us to estimate the three viscoelastic parameters of the interfacial film: τ, the characteristic time of relaxation; Ee, the equilibrium surface dilatational elasticity and Ene, the nonequilibrium part of the surface dilatational elasticity.

To describe the variation of the total interfacial tension $\Delta\gamma$, (equal to the difference between γ_i, the initial interfacial tension before the compression, and $\gamma(t)$, the interfacial tension at t time), during the time of the slow compression at a constant velocity U, we supposed that at any moment $\Delta\gamma$ can be written as a sum of equilibrium ($\Delta\gamma_e$) and nonequilibrium ($\Delta\gamma_{ne}$) contributions of stress:

$$\Delta\gamma = \Delta\gamma_e + \Delta\gamma_{ne} \quad (2)$$

The equilibrium part of the resulting stress $\Delta\gamma_e$ depends on the equilibrium elasticity *Ee*. This conservative part of elasticity is represented by the upper branch of the mechanical model in Figure 3, which corresponds to a spring. It is related to a long-range organization of the protein film and consequently to the interaction between the segments anchored at the interface.

The nonequilibrium part of the resulting stress $\Delta\gamma_{ne}$ depends on the nonequilibrium elasticity Ene and on the characteristic time of relation τ. This viscoelastic behavior is represented by the lower branch of the mechanical model in Figure 3 and corresponds to a spring coupled with a shock absorber. The nonequilibrium elasticity is linked to the dissipation of the accumulated energy through molecular reorganization like expulsion of segments in the adjacent phases occurring during the compression and the relaxation of the interface. The relaxation time τ represents the necessary time for the interface to reach a new equilibrium energetic state after a perturbation.

The two branches of the mechanical model are coupled in parallel according to eq 2, corresponding to the additivity of stresses; we obtained the following equation describing the viscoelastic behavior of the monolayer:

$$\frac{\Delta\gamma}{\Delta A}Ai = \mathrm{Ee} + \mathrm{Ene}\frac{\tau}{t}(1 - e^{-t/\tau}) \quad (3)$$

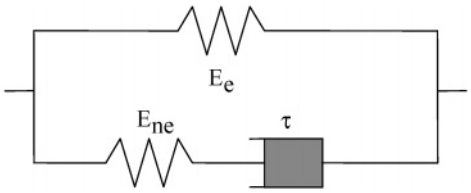

Figure 3. Mechanical model of the monolayer.

where ΔA corresponds to the drop area variation and Ai is the area of the drop before compressing the interfacial film.

The slow compression, typically lower than 0.003 s^{-1}, was performed until reaching a total relative strain ($\Delta A/Ai$) of 1−5% of the initial area, to determine the dilatational elasticity parameters. The fast compression, typically higher than 0.005 s^{-1}, was performed to determine τ.

In a pure elastic behavior (Ene = 0), we estimate Ee, which is equal to

$$\mathrm{Ee} = -Ai\frac{\mathrm{d}\gamma}{\mathrm{d}A} \tag{4}$$

Results and Discussion

1. Interfacial Tension Measurement. We have measured the γ kinetics at the H_2O-CO_2 interface at 40 °C, in the presence of OVA in the bulk water phase at concentrations ([OVA]) varying from 0.002 g/L to 4.75 g/L, and for various CO_2 pressures (50−90 bar).

We show in Figure 4 the interfacial tension profile versus CO_2 pressure obtained for the pure water−carbon dioxide system as we previously described[1], to have a better comparison with the results measured for the ovalbumin.

Furthermore, we only represent in Figure 5 some significant kinetics curves obtained in the presence of OVA in order not to complicate the text.

For an [OVA] equal to 0.002 g/L and for pCO_2 comprised between 60 and 80 bar (Figure 5A), the evolution of γ in the presence of OVA is similar to the kinetics we previously obtained for the pure CO_2-H_2O interface (Figure 4). Actually, the curve obtained for a pCO_2 of 50 bar in the presence of OVA is slightly below the curve corresponding to the pure system. Furthermore, for a pCO_2 of 90 bar (Figure 5B), the shape of the kinetics differs from that obtained for the pure interface, except for the initial rapid decrease of the interfacial tension. In particular, for 90 bar, we can notice the presence of a plateau during about 40 000 seconds, for which γ value slightly increases. This plateau is followed by a novel decrease of γ, which indicates a new organization of the interface.

From the [OVA] of 0.0229 g/L, the kinetics obtained for the pCO_2 comprised between 50 and 80 bar are different from those obtained at the pure CO_2-H_2O interface, specially for the γ equilibrium value. For 90 bar, an increase in the [OVA] to 0.0229 g/L, 0.0477 g/L, 0.523 g/L, and above, leads to a decrease of the plateau duration, which was, respectively, 8000 s, 2000 s, and unapparent.

For dilute protein solutions, the "classical" shape of kinetics at fluid interfaces is generally described as the resultant of phenomena modeled with three characteristic times.[22−26] The first time is attributed to the protein adsorption controlled by the diffusion from the bulk. The two next steps are generally related to the protein film organization via intermolecular interactions and molecular unfolding. In our case, from 60 to 80 bar, the superimposition of the kinetics acquired in the presence of OVA at 0.002 g/L with those obtained at pure CO_2-H_2O interface suggests the possibility of an inhibition of the OVA adsorption by the formation of the H_2O-CO_2 cluster network. On the other hand, increasing the [OVA] over 0.0229 g/L in this range of pCO_2 leads to kinetics becoming different from those obtained for the pure system, indicating the adsorption of the protein.

For a pCO_2 of 90 bar, the peculiar shape of the kinetics obtained for the [OVA] in the range 0.002−0.0477 g/L shows the contribution of both the CO_2 cluster formation and the OVA adsorption on the interfacial tension. The first rapid γ decrease, which looks like that obtained for the pure interface, is related to the H_2O-CO_2 organization. The presence of a plateau in the kinetics, having a duration which decreases when the [OVA] increases, reflects OVA adsorption and indicates some interaction between OVA and the H_2O-CO_2 cluster network. The fact that, at 90 bar, the protein adsorption occurs for an [OVA] of 0.002 g/L, whereas no adsorption is visible for lower pCO_2, shows an increase of the protein affinity for the interface. This could be related to the better solvatation of the CO_2-phile segments of the protein by the $ScCO_2$. This increase in affinity could also be attributed to a change in the protein conformation

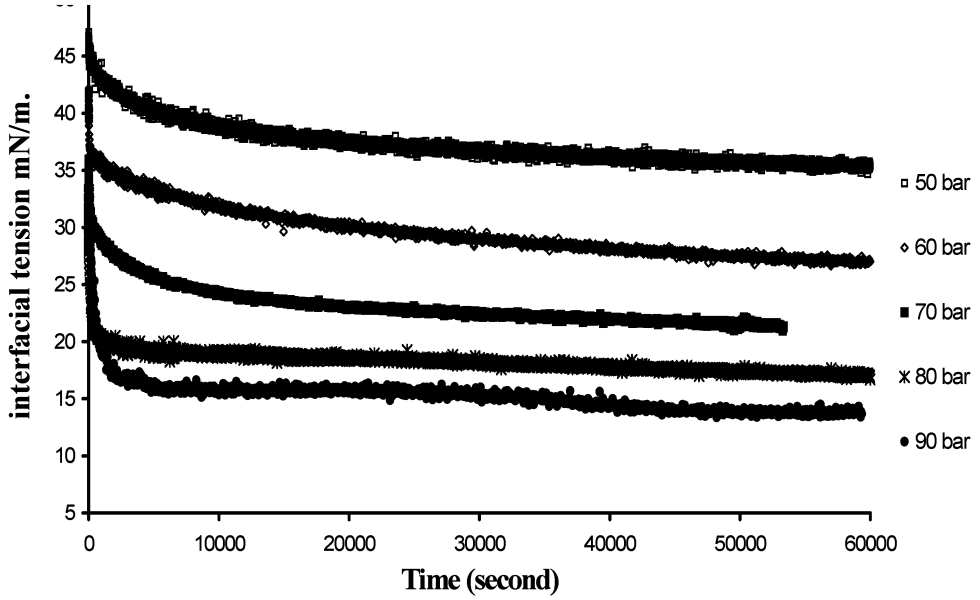

Figure 4. Interfacial tension kinetics measured at 40 °C between the pure water−CO_2 system as a function of CO_2 pressure, from Tewes et al.[1]

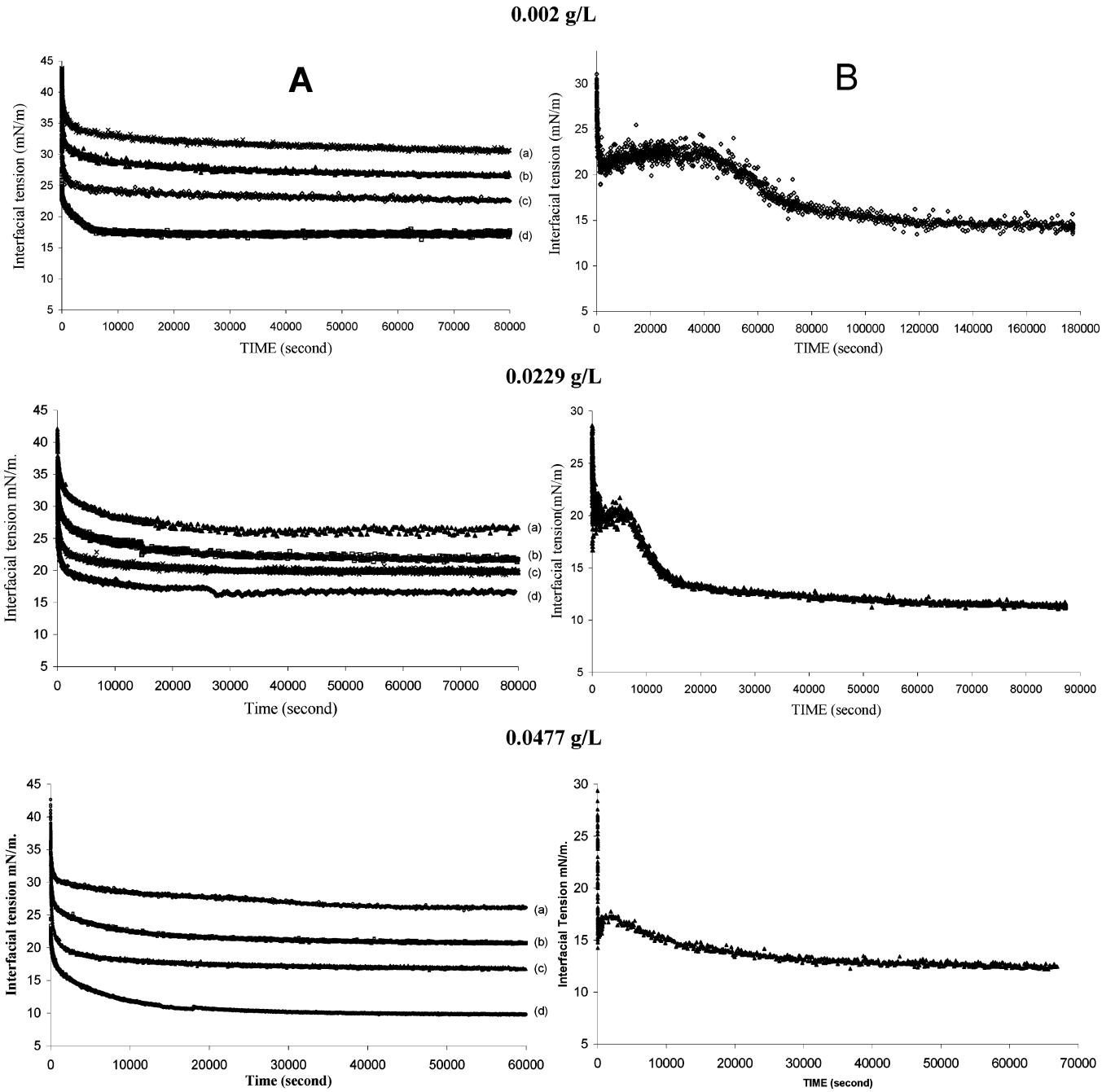

Figure 5. γ kinetics at the CO_2-H_2O interface measured at 40 °C in the presence of OVA at a concentration of 0.002 g/L, 0.0229 g/L, and 0.0477 g/L for which (A) pCO_2 was 50 bar (a), 60 bar (b), 70 bar (c), and 80 bar (d) and (B) pCO_2 was 90 bar.

for pCO_2 higher than 80 bar, as it has been shown for bovine serum albumin (BSA) and lysozyme films by FT-IR under $ScCO_2$ conditions.[27] Furthermore, the treatment of protein solutions (OVA, BSA, and myoglobin) by microbubbling of CO_2 (300 bar and 35 °C) induces an irreversible unfolding of the protein with the loss of α-helix structure.[28] This result was not only correlated with the protein denaturation due to the pH decrease, induced by the production of carbonic acid by the reaction of CO_2 with H_2O, but also with the CO_2 sorption onto the amino and guanidium protein groups.

The decrease of the duration of the plateau with the increase in [OVA] indicates that the lag time due to the protein adsorption and the development of the first intermolecular interactions decreases. At the air−water interface, a lag time of 10 000 seconds is observable on the kinetics performed with a bulk [OVA] of 0.001 g/L, and none for concentrations higher than 0.01 g/L.[29,30] In our case, the duration of the plateau is 40 000 seconds for a bulk [OVA] equal to 0.002 g/L and it is present up to a concentration of 0.0477 g/L. Therefore, for a pCO_2 of 90 bar, a peculiar phenomenon increases the necessary time for the protein to develop some interactions at the H_2O-CO_2 interface. The presence of the H_2O-CO_2 cluster network, which slows down the development of OVA−OVA interactions, combined with the required long time for the protein to modify its secondary structure under $ScCO_2$[27] could explain this result.

The slight increase of the interfacial tension during this plateau, followed by a second decrease, implies several concomitant phenomena: First, the substitution or the breaking of the cluster network by the protein, whose affinity for the interface has been increased from this pCO_2 and, second, the formation of an interfacial structure (mixed OVA−cluster or

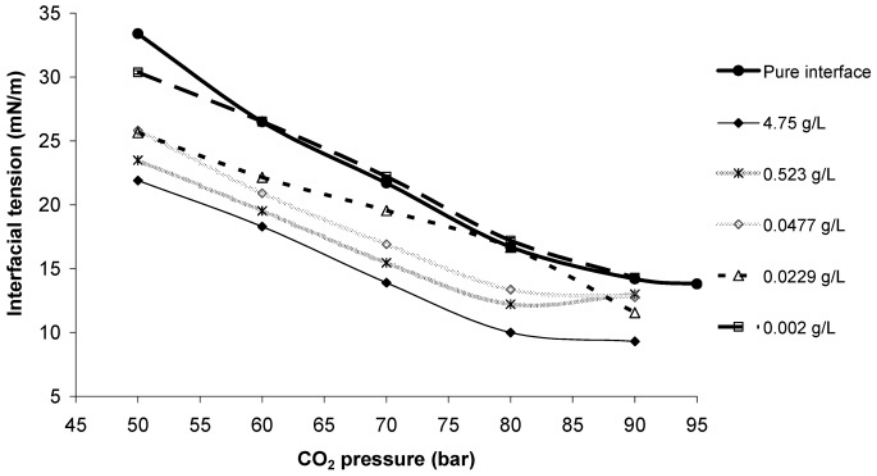

Figure 6. Variation of the equilibrium interfacial tension versus pCO_2 in the presence of various [OVA].

OVA alone), which decreases more efficiently the interfacial tension.

To analyze the interfacial layers that are formed in the different equilibrium conditions, the equilibrium γ values obtained for the several [OVA] were plotted in function of the pCO_2 (Figure 6).

Figure 6 shows three types of behavior accompanied with different organization of the interface: (i) The first behavior is observed between 60 and 80 bar and corresponds to the curves obtained for the lowest [OVA] (<0.0229 g/L). The values in these curves are very close to the γ values that we have obtained for the pure CO_2-H_2O interface. (ii) A second type of behavior is limited between 50 and 80 bar and composed of the curves obtained for the high [OVA] (0.0477−4.75 g/L), which are parallel and have very different values than those acquired for the pure interface. The curve obtained at 0.0229 g/L shows an intermediate state between behavior i and ii probably corresponding to a critical [OVA] in our system, which induces a reorganization of the protein film in the subphase. (iii) A third type of behavior includes the values acquired for a pCO_2 of 90 bar. Except for this last behavior, one can remark that the equilibrium γ values decrease when the [OVA] increases.

For an [OVA] equal to 0.002 g/L, the equilibrium γ values are equal to those obtained for the pure interface, except for the pCO_2 equal to 50 bar which gave lower values. We have shown in a previous study[1] that at 50 bar, the H_2O-CO_2 interface is slightly organized in cluster network. Then, this organization increases when the pCO_2 increases. So, for this [OVA] and a pCO_2 of 50 bar, the OVA adsorption occurs, without being obviously influenced by the organization of the H_2O and CO_2. However, above 50 bar, the equilibrium γ values suggest an inhibition of the OVA adsorption by the H_2O-CO_2 cluster network.

When we increase the [OVA] to 0.0229 g/L, the values of γ measured for the low pCO_2 (i.e., 50−70 bar) are quite different from those obtained for the pure interface, indicating a protein adsorption. However, at 80 bar γ reaches the value of the pure H_2O-CO_2 system. This can be attributed to the formation of a stronger H_2O-CO_2 cluster network that inhibits the OVA adsorption.

For the second behavior observed in Figure 6, the equilibrium γ values decrease linearly with the pCO_2 until 80 bar and the curves are parallel between them. These curves are also parallel with the curve which represents the γ values measured at time zero of the kinetics obtained for the pure H_2O-CO_2 system versus pCO_2 (Figure 1). This suggests that, from 0.0477 g/L,

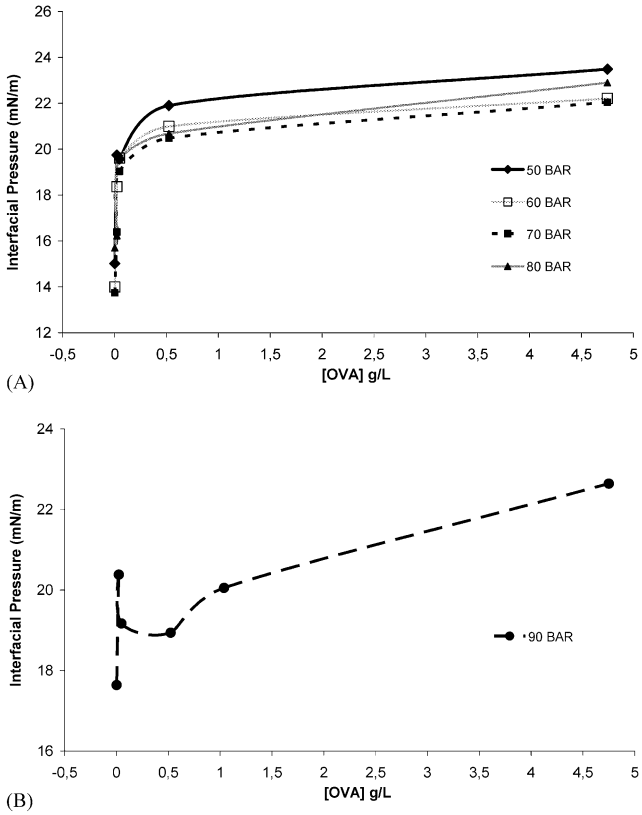

Figure 7. Interfacial pressure (π) versus OVA concentration.

the values of γ are no more influenced by the formation of a H_2O-CO_2 cluster network, but by the protein adsorption. Consequently, for high [OVA] and between 50 and 80 bar, OVA is the main component of the interfacial film.

To better describe the contribution of protein upon the adsorption phenomenon, we represented the interfacial pressure ($\pi = \gamma_0 - \gamma(t)$), where γ_0 is the initial interfacial tension and $\gamma(t)$ the interfacial tension measured at the equilibrium adsorption, in function of the [OVA] (Figure 7).

For pCO_2 comprised between 50 and 80 bar, the curves π versus [OVA] have a hyperbolic shape which is not influenced by the pCO_2 for high [OVA]. This is the shape usually found for protein adsorption at classical fluid−fluid interface,[31] or air−fluid interface, except that in our case, the pure H_2O-CO_2 interface is influenced by the H_2O-CO_2 organization leading to π values different from zero.

TABLE 1: Rheological Parameters versus pCO_2 Obtained for the Pure Interface and [OVA] Equal to 0.002 g/L

	Ee (mN/m)		Ene (mN/m)		τ (seconds)	
pCO_2 (bar)	water−CO_2	OVA 0.002 g/ L	water−CO_2	OVA 0.002 g/ L	water−CO_2	OVA 0.002 g/L
50	2 ± 1	5 ± 1	34 ± 5	19 ± 2	23 ± 8	11 ± 2
60	6 ± 1	8 ± 3	29 ± 6	8 ± 3	11 ± 4	9 ± 4
70	8 ± 3	10 ± 3	19 ± 2	18 ± 10	15 ± 8	11 ± 4
80	56 ± 19	65 ± 17	0	0	0	0
90	109 ± 12	49 ± 21	0	0	0	0

At 90 bar, the γ equilibrium values measured in the presence of a [OVA] higher than 0.002 g/L are lower than those measured for the pure interface, indicating a protein adsorption (Figure 6). However, the interfacial pressure values do not increase monotonically with the [OVA], contrary to the other pCO_2 (Figure 7B). We can observe a peculiar accident in the curve for [OVA] between 0.0229 and 0.523 g/L. Since the interfacial pressure reflects the degree of interaction between the two phases, this surprising decrease of π is probably linked to a new organization of the interfacial film, leading to a decrease of the affinity for both phases in contact (i.e., diminution of the water−CO_2 interactions). This can also be explained by the conformational state of the adsorbed protein which is controlled in part by the bulk concentration. To better precise this interfacial organization, we performed rheological measurements.

2. Rheology Measurements. We have measured the dilatational rheological comportment of the interfacial layer in the presence of various bulk [OVA] by compressing the drop area (strain) and then measuring the resulting change of γ (stress). For the pure H_2O-CO_2 interface (Table 1), the equilibrium elasticity increases with the pCO_2, leading to high elasticity values for the pCO_2 equal to 90 bar, which reveals strong lateral interactions between the H_2O-CO_2 clusters that can be compared to a solidlike behavior. In the range 50−70 bar, a viscoelastic behavior of the pure interface is observed with a significant Ene value. This can be explained by the structure of the interface, with the presence of a few number of cluster blocks surrounded by a phase made of less organized structures. The decrease of the Ene part of the elasticity with the pCO_2 indicates an organization of the interface and a lowering of the dynamic effects linked to the interaction between the cluster blocks.

At an OVA concentration of 0.002 g/L, the rheological comportment of the interface is also influenced by the pCO_2. Until a pCO_2 of 70 bar, the interfacial layer has a viscoelastic comportment, evidenced by a relaxation of the interfacial tension after the deformation is maintained (Figure 8). This behavior looks like the one we obtained at the pure interface, but with lower Ene values for 50 and 60 bar (Table 1). This last observation shows the presence of OVA intercalated between the cluster blocks. This organization could reduce the lateral motion of the blocks during the compression. At 70 and 80 bar, the rheological comportment in the presence of OVA is the same as that of H_2O-CO_2 pure system and becomes purely elastic for a pCO_2 of 80 bar. Therefore, protein adsorption is inhibited at these pressures as it was already suggested by the adsorption kinetics. These situation is depicted schematically in Figure 9.

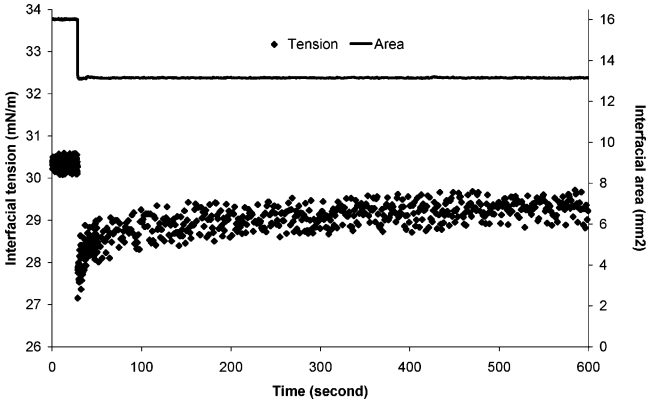

Figure 8. Fast drop compression after reaching the equilibrium state of the interfacial layer in the presence of OVA at 0.002 g/L and a pCO_2 of 50 bar.

At 90 bar, an important decrease in the equilibrium elasticity is recorded in comparison with the pure interface (Table 1, Figure 10). This indicates the presence of proteins in the interfacial film, resulting probably from the penetration of protein segments into the cluster network. This could be due to a modification of the protein conformation in the water bulk from this peculiar CO_2 pressure as already observed by Striolo et al.[27] Such comformational changes could enhance the adsorption capacity of OVA.

Another reason could be the increasing solubility of CO_2-phile protein segments into the CO_2 phase due to the increase of the density of the supercritical phase.

In presence of bulk [OVA] higher than 0.002 g/L, the interfacial layers exhibit a strict elastic comportment for all studied pCO_2. To compare the results, we have plotted the equilibrium elasticity (Ee) versus pCO_2 (Figure 10).

[OVA] higher than 0.002 g/L lead to high Ee values for the lowest pCO_2 compared to the values obtained for the pure interface. Then, in the range 0.0477−4.75 g/L of [OVA], contrary to the pure system, Ee decreases when the pCO_2 increases until 80 bar. In this range of [OVA], the more pCO_2 increases to 80 bar, the less cohesive is the interfacial layer. A decrease in Ee can be related to a decrease in the number or the energy of the interactions between the OVA segments in the plane of the interface. This can be explained by a competitive increase of the degree of interactions between the CO_2-phile segments of the OVA and the CO_2 molecules in the subphase because of the increase in the CO_2 density. By comparing adsorption and rheological properties of BSA at air/water interface and dichloromethane (DCM)/water interface, Boury et al.[14] also observed a modification of the interfacial properties, interpreted by a better partitioning of the protein segments at the liquid−liquid (DCM/water) interface. On the other hand, protein adsorption is in part entropically driven as the dehydratation of the hydrophobic segments of the protein is favored.[15] When the density of the supercritical CO_2 increases, the water−protein interactions are lowered because of the increase in the CO_2 solubility in the aqueous phase, leading to protein dehydratation and then to a change in its conformation.[28] This protein unfolding leads to the exposition of more hydrophobic segments into the water phase, which increases the affinity of the protein for the interface. Consequently, a high CO_2 density probably leads to a better partitioning of the protein between the two adjacent phases.

After 80 bar, the variation of Ee with pCO_2 is inverted, showing an increase in the cohesiveness of the interface. A

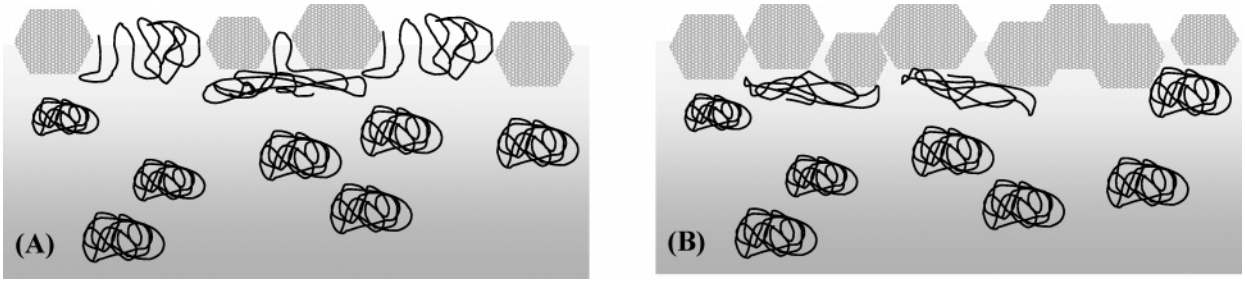

Figure 9. Schematic representation of the interfacial layer obtained at [OVA] equal to 0.002 g/L and under 50−60 bar (A) and 70−80 bar (B).

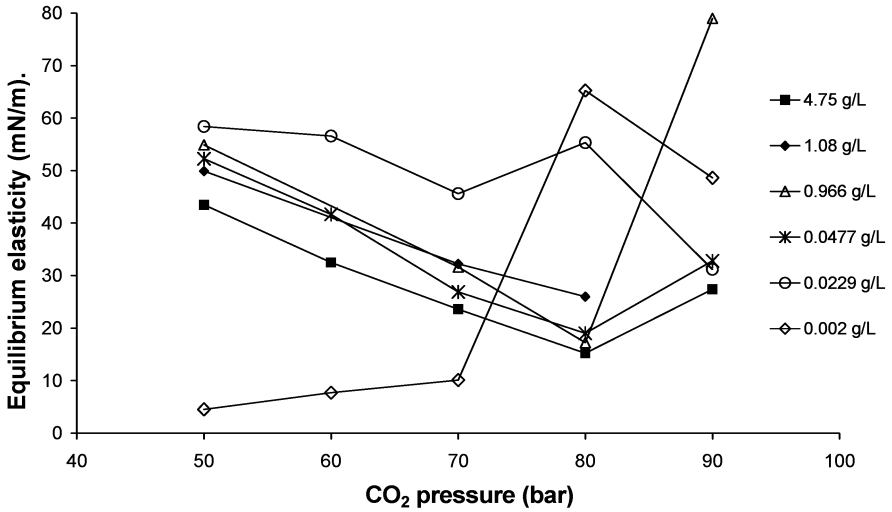

Figure 10. Equilibrium elasticity versus pCO_2 in the presence of various concentrations of OVA.

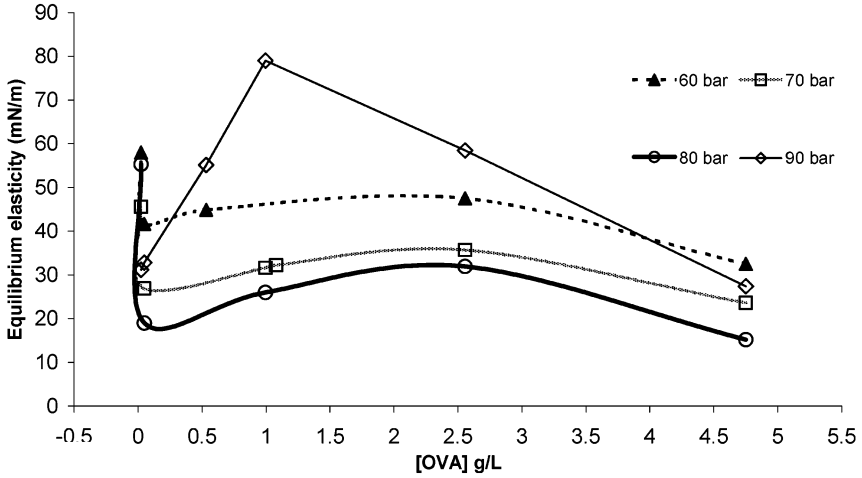

Figure 11. Equilibrium elasticity versus [OVA] concentration.

change in the OVA conformation alone cannot totally explain this increase in Ee because unfolded proteins usually give less elastic interfaces. For instance, slightly organized β-caseine gives a less elastic layer than stable lysozyme at hexadecane/water interface.[32] Therefore, additional effects must cause the formation of a peculiar layer. In fact, another reason can be the formation of a mixed layer, composed of H_2O-CO_2 clusters and OVA, in which the interactions between protein segments and clusters increase the interfacial elasticity. These clusters−protein interactions could be compared to the clathrate formed with various kind of organic compounds adsorbed onto different proteins.[33,34] Water clathrates in contact with proteins were observed earlier by the X-ray method in the Q-chymotrypsin crystals around bound *n*-hexane molecules.[35] The formation of these "protein−water−organic solvent" clathrate can induce an increase in the water uptake.[36,37] Furthermore, adsorption of CO_2 onto proteins under supercritical conditions (74 bar and 313 °K) was reported to be close to 10 wt %.[38] Thus, in our case, formation of protein$-H_2O-CO_2$ cluster probably occurs and reduces the protein dehydratation, leading to a lower partitioning between the two phases compared to that observed at 80 bar, explaining the increase in Ee.

To interpret the effect of [OVA] on the elasticity behavior of the interface, we represented Ee versus the [OVA] for different CO_2 pressures. We have plotted the values measured for [OVA] higher than 0.002 g/L, since at this pressure the protein adsorption did not occur. At pressures lower than 90 bar, Ee is maximum for the lowest [OVA]. Then, Ee abruptly decreases and slightly evolves with the concentration. The effect of the concentration on the interfacial equilibrium elasticity could be explained as it was previously done at the dichloromethane/water interface in the presence of BSA.[14] At low

protein concentrations, the interfacial molecular area is high and the protein is greatly unfolded. This allows the anchored segments to maximize their lateral interactions, explaining the strong elastic behavior. At high protein concentrations, proteins at the interface are less unfolded, promoting intramolecular interactions rather than interactions between the anchored segments

For 90 bar, the comportment of Ee versus protein concentration is different to that obtained for the other pressures. Ee increases strongly and linearly with the [OVA] until 1 g/L, and then it decreases. This increase in Ee shows an increase of the interface cohesiveness and it is concomitant with the accident observed on the $\pi-$[OVA] curve (Figure 7B). This increase in Ee can be due to a poor partitioning of the protein through the two adjacent phases because of the interactions with the H_2O-CO_2 clusters reducing the protein dehydratation. Finally, the interactions of the clusters with the protein modulate the degree of the water$-CO_2$ interaction and lead to a decrease in the interfacial pressure. At low protein concentrations, the time for the proteins to reach the interface is high and the clusters have enough time to form, allowing their further interaction with the protein. At high protein concentrations (above 1 g/L), proteins can saturate the interface before the initiation of the cluster formation.

Conclusion

We demonstrated that protein interfacial layers formed at CO_2-water interface can be analyzed by means of a pendant drop technique. This technique allowed us to measure the adsorption kinetics and dilatational properties of the films. Results show that OVA adsorption is inhibited by H_2O-CO_2 cluster formation for a bulk concentration of 0.002 g/L and for pCO_2 comprised between 50 and 80 bar. For higher concentration, and in these ranges of pCO_2, OVA is able to adsorb with an organization pCO_2 dependent. Moreover, for a pCO_2 of 90 bar, and for all OVA concentrations, we obtained peculiar effects probably related to the formation of mixed films made of protein and H_2O-CO_2 clusters.

This complex adsorption process involves four main phenomena which are dependent on pressure and protein concentration: (i) the formation of a cluster network at the H_2O-CO_2 interface, (ii) the adsorption of proteins involving classical mechanisms such as unfolding and multilayer formation, (iii) the solvatation properties of the CO_2 toward protein segments, and (iv) the conformational modifications of the protein molecules in the bulk water.

Our results show that, for H_2O-CO_2 interfacial studies performed in the presence of macromolecular surfactant, the formation of water$-CO_2$ network should be taken into account.

Proteins could be good candidates to create a cohesive film at the H_2O-CO_2 interface, which may be useful to inhibit the coalescence of water droplets in a CO_2 surrounding phase (inverse emulsions). Studies are in course to establish the ability of protein to stabilize such emulsions. This involves feasibility diagrams and analysis of the structural conformation of the proteins in emulsion, in particular by Raman spectroscopy.

References and Notes

(1) Tewes, F.; Boury, F. *J. Phys. Chem. B* **2004**, *108*, 2405.
(2) Teng, H.; Yamasaki, A. *Int. J. Heat Mass Transfer* **1998**, *41*, 3204.
(3) Jacobson, G. B.; Lee, C. T., Jr.; Johnston, K. P.; Tumas, W. *J. Am. Chem. Soc.* **1999**, *121*, 11902.
(4) Kane, M. A.; Baker, G. A.; Pandey, S.; Bright, F. V. *Langmuir* **2000**, *16*, 4901.
(5) da Rocha, S. R. P.; Harrison, K. L.; Johnston, K. P. *Langmuir* **1999**, *15*, 419.
(6) Holmes, J. D.; Bhargava, P. A.; Korgel, B. A.; Johnston, K. P. *Langmuir* **1999**, *15*, 6613.
(7) Eastoe, J.; Bayazit, Z.; Martel, S.; Steytler, D. C.; Heenan, R. K. *Langmuir* **1996**, *12*, 1423.
(8) Harrison, K.; Goveas, J.; Johnston, K. P.; O'Rear, E. A. *Langmuir* **1994**, *10*, 3536.
(9) Campbell, M. L.; Apodaca, D. L.; Yates, M. Z.; McCleskey, T. M.; Birnbaum, E. R. *Langmuir* **2001**, *17*, 5458.
(10) Chun, B.-S.; Wilkinson, G. T. *Ind. Eng. Chem. Res.* **1995**, *34*, 4371.
(11) Psathas, P. A.; Janowiak, M. L.; Garcia-Rubio, L. H.; Johnston, K. P. *Langmuir* **2002**, *18*, 3039.
(12) Eastoe, J.; Dupont, A.; Steytler, D. C. *Curr. Opin. Colloid Interface Sci.* **2003**, *8*, 267.
(13) Bos, A. M.; van Vliet, T. *Adv. Colloid Interface Sci.* **2001**, *91*, 437.
(14) Boury, F.; Ivanova, T.; Panaieotov, I.; Proust, J. E.; Bois, A.; Richou, J. *Langmuir* **1995**, *11*, 1636.
(15) Renault, A.; Pezennec, S.; Gauthier, F.; Vié, V.; Desbat, B. *Langmuir* **2002**, *18*, 6887.
(16) Da Rocha, S. R. P.; Johnston, K. P.; Westacott, R. E.; Rossky, P. J. *J. Phys. Chem. B* **2001**, *105*, 12092.
(17) Sloan, E. D. *Clathrate hydrates of natural gases*, 2nd ed.; Marcel Dekker: New York, 1998.
(18) Mori, Y. H. *Energy Convers. Mgmt.* **1998**, *39*, 1537.
(19) Saulnier, P.; Boury, F.; Malzert, A.; Heurtault, B.; Ivanova, T.; Cagna, A.; Panaïotov, I.; Proust, J. E. *Langmuir* **2001**, *17*, 8104.
(20) Malzert, A.; Boury, F.; Saulnier, P.; Benoît, J. P.; Proust, J. E. *Langmuir* **2002**, *18*, 10248.
(21) Panaiotov, I.; Ivanova, T.; Proust, J.; Boury, F.; Denizot, B.; Keough, K.; Taneva, S. *Colloids Surf., B: Biointerfaces* **1996**, *6*, 243.
(22) Beverung, C. J.; Radke, C. J.; Blanch, H. W. *Biophys. Chem.* **1999**, *81*, 59.
(23) Kiss, E.; Borbas, R. *Colloids Surf., B: Biointerfaces* **2003**, *31*, 169.
(24) Ybert, C.; di Meglio, J.-M. *Langmuir* **1998**, *14*, 471.
(25) Fainerman, V. B.; Lucassen-Reynders, E. H.; Miller, R. *Adv. Colloid Interface Sci.* **2003**, *106*, 237.
(26) Fang, F.; Szleifer, I. *Biophys. J.* **2001**, *80*, 2568−2589.
(27) Striolo, A.; Favaro, A.; Elvassore, N.; Bertucco, A.; Di Noto, V. *J. Supercrit. Fluids* **2003**, *27*, 283.
(28) Ishikawa, H.; Shimoda, M.; Yonekura, A.; Mishima, K.; Matsumoto, K.; Osajima, Y. *J. Agric. Food Chem.* **2000**, *48*, 4535.
(29) Gauthier, F. Contribution à l'étude de l'adsorption de protéines aux interfaces. Ph-D, Université Joseph Fourier - Grenoble I, 2000.
(30) Pezennec, S.; Gauthier, F.; Alonso, C.; Graner, F.; Croguennec, T.; Brule, G.; Renault, A. *Food Hydrocolloids* **2000**, *14*, 463.
(31) Chen, P.; Lahooti, S.; Policova, Z.; Cabrerizo-Vilchez, M. A.; Neumann, A. W. *Colloids Surf., B: Biointerfaces* **1996**, *6*, 279.
(32) Freer, E. M.; Yim, K. S.; Fuller, G. G.; Radke, C. J. *J. Phys. Chem. B* **2004**, *108*, 3835.
(33) Phillips, J. B.; Nguyen, H.; John, V. T. *Biotechnol. Prog.* **1991**, *7*, 43.
(34) Gorbatchuk, V. V.; Ziganshin, M. A.; Mironov, N. A.; Solomonov, B. N. *Biochim. Biophys. Acta (BBA) − Protein Structure and Molecular Enzymology* **2001**, *1545*, 326.
(35) Yennawar, N. H.; Yennawar, H. P.; Farber, G. K. *Biochemistry* **1994**, *33*, 7326.
(36) Sirotkin, V. A.; Borisover, M. D.; Solomonov, B. N. *Biophys. Chem.* **1997**, *69*, 239.
(37) Gorbatchuk, V. V.; Mironov, N. A.; Solomonov, B. N.; Habicher, W. D. *Biomacromolecules* **2004**, *5*, 1615.
(38) Nakanura, K.; Hoshino, T.; Ariyama, H. *Biosci. Biotechnol. Biochem.* **1991**, *30*, 2341.